Catalysis Today 160 (2011) 144–152

Contents lists available at ScienceDirect

Catalysis Today

journal homepage: www.elsevier.com/locate/cattod

Enhance catalytic activity for CO oxidation over titania supported gold catalysts that dispersed on SiO_2

Zhao-Wen Wang, Xin V. Wang, D. Ying Zeng, Ming-Shu Chen*, Hui-Lin Wan

State Key Laboratory of Physical Chemistry of Solid Surfaces, National Engineering Laboratory for Green Chemical Productions of Alcohols-Ethers-Esters, Department of Chemistry, College of Chemistry and Chemical Engineering, Xiamen University, Xiamen, 361005 Fujian, China

ARTICLE INFO

Article history:
Available online 3 August 2010

Keywords:
Gold
Titania
TiO_2–SiO_2
Nanocatalysis
CO oxidation

ABSTRACT

The enhanced dispersion of gold on TiO_2 was achieved by dispersing TiO_2 onto a high-surface-area SiO_2 powder support. High temperature reduction, at 773–873 K, in hydrogen leads to very active gold nanoparticles on the support surfaces for CO oxidation at room temperature. The surface sol–gel method results better dispersion for both TiO_2 and Au, and higher activity for CO oxidation than that by the conventional impregnation method. Metallic gold with slightly negative charge was evidenced by X-ray photoelectron spectroscopy (XPS) and *in situ* transmission infrared spectroscopy (FTIR) using CO as a probe. The obtained $Au/TiO_2/SiO_2$ catalysts show better stability and higher activities for CO oxidation than that for Au/TiO_2. The promotion effects may origin from the formation of thin layer and small crystalline particles of TiO_2 anchored on SiO_2, leading to a better dispersion of small Au nanoparticles and sinter resisting.

1. Introduction

The interest in studying supported Au catalysts has increased substantially since Haruta and Hutchings showed extraordinary catalytic properties in some reactions [1,2]. Although, Au was reported to be active for CO oxidation on 1925 and 1975 [3,4]. Haruta et al. [1] found that gold nanoparticles deposited on reductive metal oxides exhibit high catalytic activity for low temperature CO oxidation. Hutchings and co-workers [2] found that gold catalysts are catalytically active for hydrochlorination of acetylene to vinyl chloride. Supported gold catalysts have been found to be active for several important reactions like epoxidation of propene [5,6], reduction of nitrogen oxides [7,8], water gas shift reaction [9], low temperature CO oxidation [1,3,4,10–12], and many selective oxidation or hydrogenation of fine chemical [13,14].

Most of the experimental and theoretical studies to date have focused on understanding the origin of the unique activity for low temperature CO oxidation and the issues have been addressed extensively. These studies have concluded that the unique catalytic activity is related to the properties of the metal oxide supports [15], defects on the oxide surface [16,17], quantum size effect with respect to the size of Au nanoparticles [10,18–20], effect of the size of gold particles [11], the structures of the interface of Au nanoparticles and oxide support surfaces [21], and the details in the preparation procedure [22,23]. While how to retain the high activity of Au catalysts remains unsolved, which limits its commercialized applications. It was found that the catalytic activity for CO oxidation on $Au/TiO_2(1\,1\,0)$ decreases sharply within 2 h due to the conglomeration of Au nanoparticles. Such rapid sintering of Au nanoparticles under reaction condition was attributed to quenching of the surface oxygen vacancies on TiO_2 which weakens the binding energy of Au with TiO_2 [10,24].

In order to suppress the sintering of Au nanoparticles under the reaction condition or thermal treatment at high temperature, one of the strategies is to confine them into porous materials forming a core–shell structure [25]. Zheng et al. have recently prepared yolk–shell particles with 6.3 nm Au nanoparticles core and ZrO_2 or TiO_2 mesoporous shell [26]. Another strategy is to find a suitable substrate capable of efficiently stabilizing supported Au nanoparticles through the strong metal support interaction (SMSI). Adding a third component had been found to enhance the catalytic activity significantly [27–42]. Yan et al. [32] experimentally demonstrated that deposition of Au nanoparticles on a nanocrystalline TiO_2 modified with aluminum oxide can enhance stability of supported Au nanocatalysts. The amorphous aluminum oxide layer was found to play an extremely important role in the stabilization of the supported Au nanoparticles without affecting catalytic activities. Huang and co-workers [33] had shown that Au species have a strong interaction with highly dispersive CeO_2 deposited on SiO_2. Goodman et al. [19,34] had reported the stabilization of highly active Au nanoparticles by surface defects via substituting Ti atom for Si in a silica thin film network. A novel design of gold catalysts with enhanced thermal stability by post-modification of Au/TiO_2 by amorphous SiO_2 decoration has been reported [35].

* Corresponding author. Tel.: +86 592 2183723; fax: +86 592 2183047.
E-mail address: chenms@xmu.edu.cn (M.-S. Chen).

0920-5861/$ – see front matter © 2010 Elsevier B.V. All rights reserved.
doi:10.1016/j.cattod.2010.07.006

Studies at ultrahigh vacuum condition showed that the Au bilayer structure deposited on a reduced titania thin film grown on Mo(1 1 2) [20], (Mo(1 1 2)–(8 × 2)-TiO*x*), is exceptionally active. The binding energy of Au and Ti^{4+} is apparently higher than that of Au–Au according to TPD of Au [17], which enables Au nanoparticles to be stable on the support. Inspired from this, one to a few layers of TiO_2 coating on another oxide support surface would be expected to have a stronger interaction with Au atoms. In the present work, we have deposited Au nanoparticles on TiO_2 that dispersed on SiO_2 prepared by a conventional impregnation method and a surface sol–gel method. Such dispersion enhances the stability of Au nanoparticles. Furthermore, the activities for CO oxidation are much higher as compared to that for Au on TiO_2.

2. Experimental

2.1. Catalyst preparation

A commercial high-surface area silica (specific surface area = 400 m^2/g) was used as a support. The silica support was cleaned by soaking overnight in 30% HNO_3 solution, washed with distilled water, then dried at 110 °C and calcined at 550 °C for 2 h before use. TiO_2/SiO_2 mixed oxides were prepared by a surface sol–gel (SSG) process and a conventional impregnation method. The procedure of SSG for coating monolayer to multilayer titanium oxide and other metal oxide films onto a silica surface was developed according to the method described by Kunitake and co-workers [43], which is similar to grafting titanium alkoxides on SiO_2 [44]. In the present work, 10 g of the pre-cleaned high-surface area SiO_2 powder sample was dried in flowing Ar at 130 °C for 11 h, and then loaded into a reflux bottle. Subsequently, a solution of tetrabutyl titanate (11 mL), Ti-(O-n-Bu)$_4$, in anhydrous toluene (110 mL) was added, following vigorous reflux at the boiling temperature of toluene (112 °C) for 4 h. Then the sample was filtered, washed several times with anhydrous ethanol and toluene respectively, and dried at 130 °C for 2 h, hydrolyzed with steam at 80 °C, and finally dried at 130 °C for 2 h again. In order to cover the silica surface with TiO_2 completely, the procedure of grafting was repeated several times. The final TiO_2/SiO_2 samples were calcined in air at 500 °C for 2 h. Here after the obtained samples were denoted as T-*N*-S, in which *N* stands for the repeating number. In the second method (a conventional impregnation method, IMP), silica was immersed in certain amount of $TiCl_3$–HCl solution for 12 h, then dried and calcined at 500 °C for 2 h. The obtained samples were described as *x* wt% TS according to the TiO_2 loading. For comparison, TiO_2/SiO_2 was also prepared by IMP method using $Ti(OC_4H_9)_4$ as a precursor.

Au was deposited onto the above prepared supports by an IMP method using chloroauric acid ($HAuCl_4$) as a precursor. The paste was dried at ~323 K first, at 373 K then for overnight. The obtained precursor was then reduced in hydrogen at temperature between 523 and 973 K. The catalysts after reduction were purged by helium, then directly exposed to CO:O_2:He (1:1:98) mixture without exposing to air. Space velocity is controlled at 600,000 mL per g-catalyst per hour.

2.2. Catalytic testing

The CO oxidation reaction was carried out in a U-tube quartz reactor with a water bath to better control the reaction temperature. Typically, 10 mg of catalyst was used. Samples were reduced in a vertical fixed-bed quartz reactor using high-purity H_2. Then the catalyst was transferred into the U-tube reactor under the protection of high-purity He. Reaction gas of 1 vol.% CO and 1 vol.% O_2 balanced with He, pre-purified by a liquid N_2 trap, was flowed at an ambient pressure through the catalyst at a rate of 30 mL/min. The reaction products were analyzed using a gas chromatograph (GC) equipped with a methanation convertor and a flame ionization detector (FID).

2.3. Catalyst characterization

The diffusion reflectance UV–vis (DR-UV–vis) spectra were taken on a Varian Cary-5000 spectrometer equipped with a diffuse-reflectance accessory. The spectra were collected with dehydrated $BaSO_4$ as a reference and recorded in the diffused reflectance mode (*R*) and transformed to a Kubelke-Munk function (*F*(*R*)).

The powder X-ray diffraction (XRD) patterns for the structure determination were measured on a Phillips Panalytical X'pert Pro diffractometer equipped with a graphite monochromator. Cu K_α radiation (40 kV and 30 mA) was used as the X-ray source.

The X-ray photoelectron spectroscopy (XPS) was measured with a PHI Quantum 2000 Scanning ESCA Microprobe equipment (physical Electronics) using monochromatic Al K_α radiation ($h\nu$ = 1486.6 eV). The background pressure in the analysis chamber was lower than 1×10^{-7} Pa. The X-ray beam diameter was 100 μm, and the pass energy was 58.7 eV for each analysis. All binding energies were referenced to the C 1s hydrocarbon peak at 284.6 eV.

Nitrogen physisorption at 77 K was carried out with a Micromeritics Tristar 3000 surface area and porosimeter analyzer to examine the surface area and the porous property of each sample. The samples were pretreated at 573 K in vacuum for 3 h before N_2 adsorption. The specific surface area was calculated following the BET method. The pore diameter distribution was evaluated by the BJH method according to the desorption isotherm branch.

The prepared fresh and used catalyst samples were characterized using X-ray photoemission spectroscopy (XPS, Quantum 2000), transmission electron microscope (TEM, FEI Tecnai 300 kV), and *in situ* Fourier transmission infrared spectroscopy (FTIR, Nicolet Nexus 870) combined with home-made *in situ* IR cell [45].

3. Results and discussion

3.1. Catalyst performance

The catalytic activities for CO oxidation over 2 wt% Au supported on TiO_2/SiO_2 prepared by the surface sol–gel (SSG) and conventional impregnation (IMP) methods as a function of the reduction temperature were compared with that on TiO_2 in Fig. 1. It clearly shows the significant effects of the reduction temperature on the

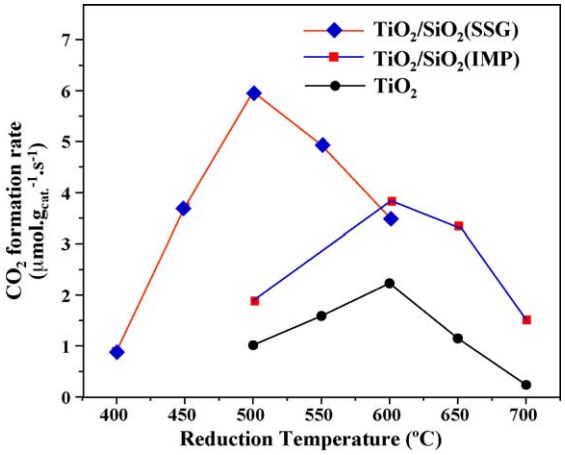

Fig. 1. Catalytic activities for CO oxidation over 2 wt% Au/TiO_2 and Au/TiO_2/SiO_2 prepared both by the SSG and IMP as a function of the reduction temperature.

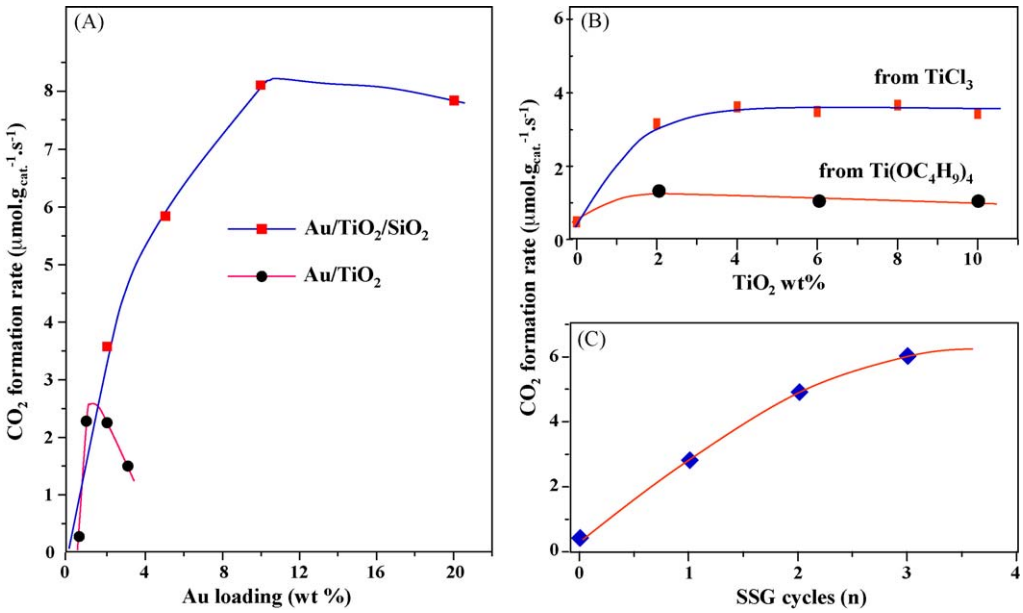

Fig. 2. (A) Catalytic activities for CO oxidation over TiO_2 and TiO_2/SiO_2 supported Au catalysts (IMP method) as a function of Au loading; (B) catalytic activities for CO oxidation over 2 wt% $Au/TiO_2/SiO_2$ as a function of TiO_2 loading, where the TiO_2/SiO_2 supports were prepared by the IMP method using $TiCl_3$ and $Ti(OC_4H_9)_4$ as a precursor, respectively; (C) catalytic activities for CO oxidation over 2 wt% $Au/TiO_2/SiO_2$ as a function of the cycle number for coating TiO_2 onto SiO_2 by SSG method.

catalytic activities for the all three oxide supports. The best reduction temperatures to achieve the highest catalytic activities are 600 °C for 2 wt% Au on both TiO_2 and 10 wt TiO_2/SiO_2 (IMP), but 500 °C for that on TiO_2/SiO_2 (SSG). The results also illustrate significant promotion effects of the TiO_2 that dispersed on SiO_2, with CO_2 formation rate on TiO_2/SiO_2 (SSG) being about three times higher than that on TiO_2 and more than an order higher than that on SiO_2.

The promotional effects of TiO_2 dispersion can also be seen in the Au loading as shown in Fig. 2(A). The highest reaction rate of about 2.5 μmol CO_2 per gram catalyst per second appears at 2 wt% Au loading on TiO_2, while the rate continuously increases up to 8 μmol CO_2 g_{cat}^{-1} s^{-1} as the Au loading up to 10 wt% on the TiO_2/SiO_2 (IMP). For a 2 wt% Au loading, the catalytic activity achieves almost a constant value of 3.6 μmol g_{cat}^{-1} s^{-1} after TiO_2 dispersed amount higher than 4 wt% by the IMP method (Fig. 2(B)), while continuously increases up to more than 6 μmol g_{cat}^{-1} s^{-1} at the third cycles of TiO_2 coating by the SSG method (Fig. 2(C)).

3.2. Catalyst characterization

3.2.1. Diffuse-reflectance-UV–vis spectroscopy

DR-UV–vis spectroscopy is a very useful tool to investigate the band structure of TiO_2, as well as oxide supported TiO_2 and its mixed oxides. It also provides some useful information on the coordination geometry of Ti cation. Blue shifts of the absorption edge have been observed due to the quantum size effect [46] and the changes of the coordination configuration of Ti [47]. The DR-UV–vis spectra of the prepared TiO_2/SiO_2 supports by IMP and SSG methods are compared with the commercial TiO_2 and SiO_2 in Fig. 3(A) and (C). It is obvious that all the prepared TiO_2/SiO_2 samples show a band at ~230 nm, which is a typical band of the Ti cation in a tetrahedral coordination. The octahedral coordination featured with a band at ~320 nm [46,47], especially for the sample prepared by IMP with TiO_2 loading higher than 4 wt%. The slightly narrower feature and stronger intensity (respective to that of TiO_2) for the sample prepared by SSG than those for IMP may suggest a more unique dispersion of TiO_2 on SiO_2 by using SSG. Note that Ti^{4+} takes an octahedral coordination geometry in a bulk TiO_2, while it is popular for a tetrahedral coordination for surface TiO_2 and highly dispersive Ti^{4+} in a SiO_2 framework. Supporting of gold using chloroauric acid ($HAuCl_4$) as a precursor following a high temperature reduction under hydrogen does not cause obvious change of the DR-UV–vis band features for both two types of supports prepared by the IMP and SSG methods, see Fig. 3(B) and (D).

3.2.2. XRD examination

XRD analyses were conducted on all the prepared supports with and without gold to characterize the dispersion and structure of surface TiO_2. The obtained XRD patterns are shown in Figs. 4 and 5. A broad peak at 2θ of 15–30° was observed for the samples prepared by both of the IMP and SSG, which can be assigned to the amorphous framework of SiO_2. For TiO_2/SiO_2 samples prepared by the IMP method using $TiCl_3$ as a precursor (Fig. 4(A)), a group of sharp peaks corresponding to the rutile TiO_2 appear for the TiO_2 loading higher than 4 wt%. This implies that beside a part of TiO_2 highly disperses on the SiO_2 surface, the other part of TiO_2 forms crystalline rutile on the surfaces, consistent with DR-UV–vis results. The TiO_2/SiO_2 samples prepared by the SSG method using $Ti(OC_4H_9)_4$ as a precursor show only the broad feature characterized of amorphous SiO_2 (Fig. 5(B)), which confirms a better dispersion of TiO_2 on the SiO_2 support as shown by DR-UV–vis. In contrast, the TiO_2/SiO_2 samples prepared by the IMP method using $Ti(OC_4H_9)_4$ as a precursor (Fig. 4(C)) forms anatase TiO_2. Here we would like to emphasize that the dispersion of TiO_2 onto SiO_2 using SSG was confirmed by DR-UV–vis and XPS which detail will be discussed in the next section. Thus, it can be concluded that TiO_2 is highly dispersive on the SiO_2 surface without forming crystalline TiO_2 phase by SSG.

Fig. 5(A) showed XRD pattern of the TiO_2 support, which is mainly characterized as an anatase phase. For the 10 wt% TiO_2/SiO_2, after supporting of 2 wt% Au, the peaks corresponding to the rutile become sharper and XRD peaks corresponding to gold particles appear (Fig. 5(B)). While impregnation of 2 wt% of Au onto the TiO_2/SiO_2 prepared by SSG, a set of weak XRD peaks corresponding to anatase TiO_2 appear, together with a set of sharp peaks for Au crystalline particles. Such results reveal that the well coating TiO_2

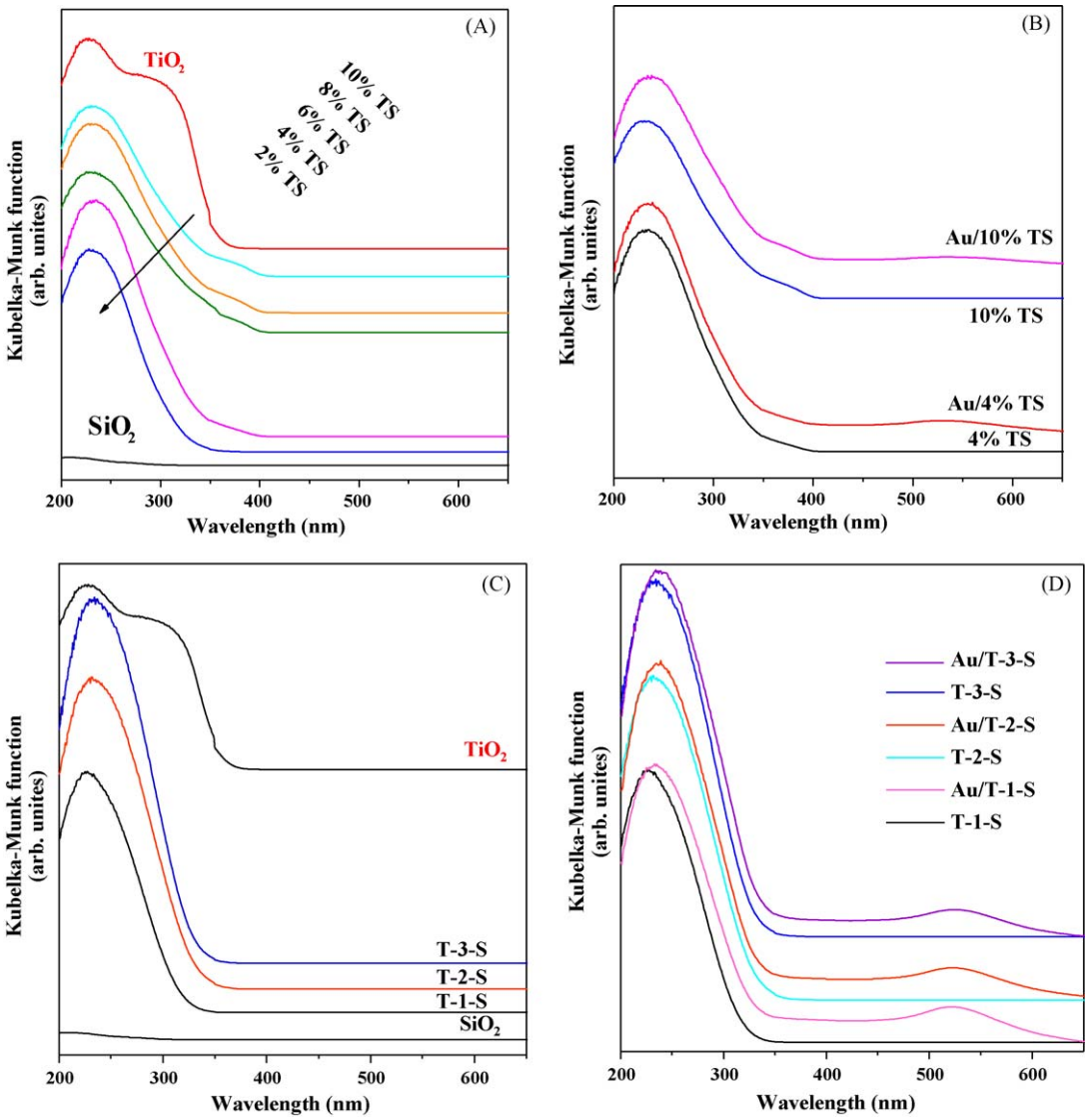

Fig. 3. DR-UV–vis spectra: (A) TiO_2/SiO_2 supports prepared by the IMP method with different TiO_2 loading; (B) comparison of TiO_2/SiO_2 supports prepared by the IMP and after 2 wt% Au loading; (C) TiO_2/SiO_2 supports prepared by the SSG method with different repeating cycles; (D) comparison of TiO_2/SiO_2 supports prepared by the SSG and after 2 wt% Au loading.

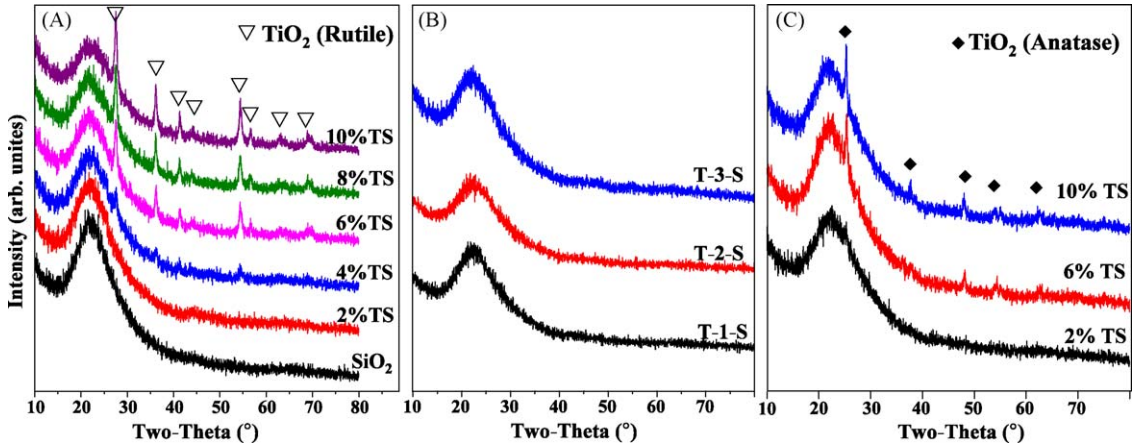

Fig. 4. XRD patterns of TiO_2/SiO_2 supports with different TiO_2 loading prepared by (A) IMP method using $TiCl_3$ as a precursor, (B) SSG method using $Ti(OC_4H_9)_4$ as a precursor, and (C) IMP method using $Ti(OC_4H_9)_4$ as a precursor.

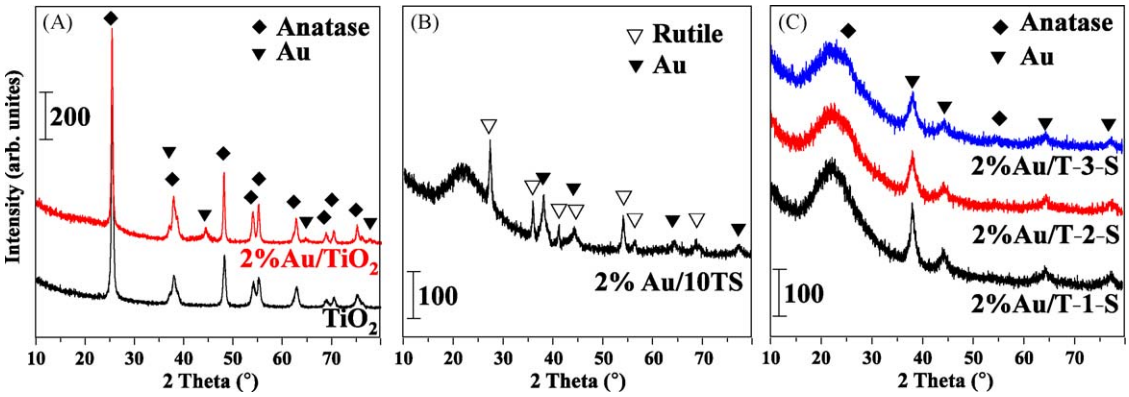

Fig. 5. XRD patterns of (A) TiO_2 support and 2 wt% Au/TiO_2, (B) 2 wt% Au/10 wt% TiO_2/SiO_2 (IMP), (C) 2 wt% Au/TiO_2/SiO_2, which supports TiO_2/SiO_2 were prepared by the SSG method with different coating cycles.

films on the SiO_2 were partially mangled forming crystalline TiO_2 particles.

3.2.3. XPS measurement

Further characterization of the dispersion of TiO_2 on SiO_2 prepared by both SSG and IMP method were performed by XPS. Fig. 6 shows XPS profiles of the Ti 2p and O 1s for the different samples. The binding energies (BE) of Si 2p for all the samples are well identical with that for the SiO_2 support. The Ti $2p_{3/2}$ binding energy for the samples prepared by IMP is found at ~458.8 eV for TiO_2 loading of 2 wt%, and red-shifts to 458.3 eV with TiO_2 loading higher than 4 wt%. This binding energy of 458.3 eV is identical with that observed for the mechanical mixture of TiO_2 and SiO_2, and in well agreement with the reference value of Ti^{4+} (458–459 eV) [48,49]. An apparent higher binding energy of 459.2 eV is observed for TiO_2/SiO_2 prepared by the SSG process. A blue-shift of 0.5–1.9 eV for the Ti $2p_{2/3}$ peak had been reported for the highly dispersive TiO_2 on SiO_2, which is supposed to be due to the formation of

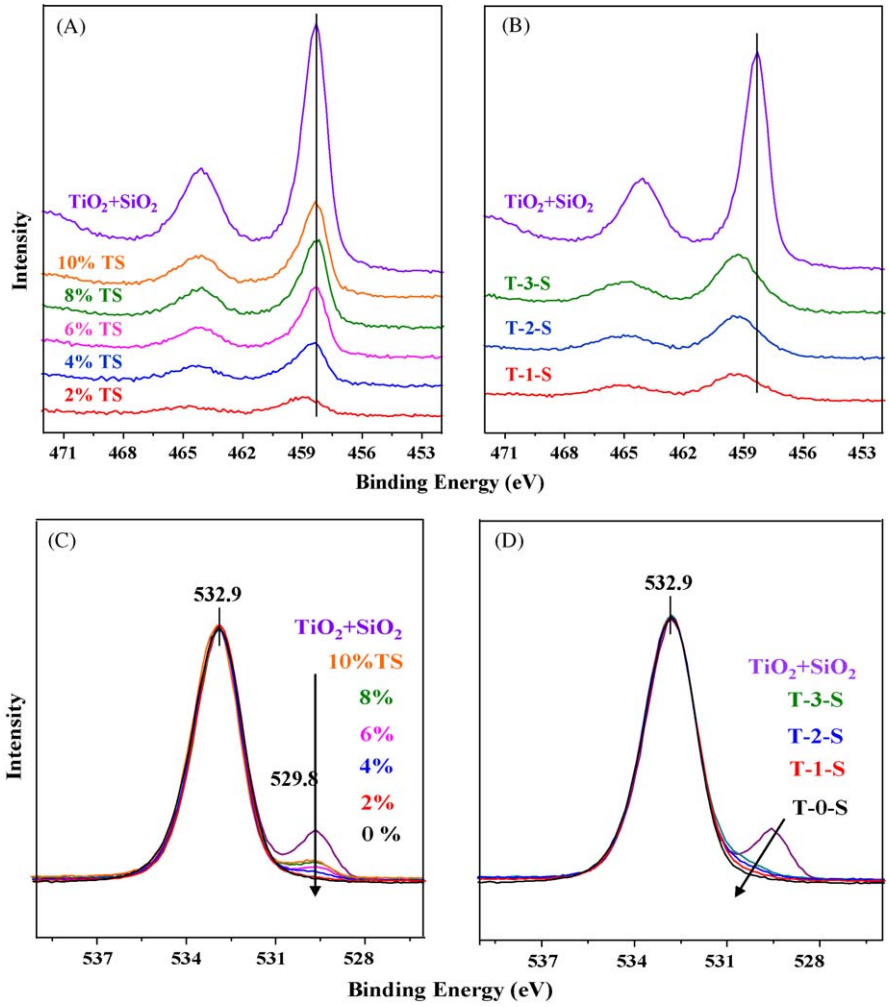

Fig. 6. XPS spectra of various TiO_2/SiO_2 supports and a mechanical mixture of TiO_2 and SiO_2: (A) Ti 2p for the samples prepared by the IMP method, (B) Ti 2p for the samples prepared by the SSG method, (C) O 1s for the samples prepared by the IMP method, and (D) O 1s for the samples prepared by the SSG method.

Table 1
Physical properties of various supports derived from N_2 physisorption and XPS analysis.

Supports	Surface area (m^2/g)	Pore volume (cm^3/g)	XPS ratio of Ti 2p/Si 2P
TiO_2	139	–	–
SiO_2	398	0.91	–
2% TS	382	0.87	0.013
4% TS	371	0.81	0.028
6% TS	359	0.78	0.042
8% TS	338	0.75	0.057
10% TS	332	0.75	0.059
T-1-S	392	0.73	0.032
T-2-S	388	0.70	0.047
T-3-S	385	0.67	0.063

Ti–O–Si linkages [49,50]. Since Ti atom is less electronegative than Si, the formation of the Ti–O–Si linkages will lead to a more positive charge on Ti^{4+} and results the blue shift of Ti 2p peaks.

The formation of Ti–O–Si linkages is evidenced by a shoulder at the lower binding energy side of the O 1s for SiO_2, which binding energy is higher than that of TiO_2 (Fig. 6(C) and (D)). The binding energies of O 1s for TiO_2 and SiO_2 are well identified at 529.8 and 532.9 eV respectively, using a sample of TiO_2 and SiO_2 mixture. The TiO_2/SiO_2 prepared by the IMP method appears a small peak at about 530 eV for the O 1s, which is well separate from that of SiO_2. However, only a small shoulder at the lower binding energy side of the O 1s for SiO_2 is observed for TiO_2/SiO_2 prepared by the SSG method. Such results reveal that TiO_2 disperses better on SiO_2 prepared by SSG than by IMP. Crystalline TiO_2 forms on SiO_2 prepared by IMP, especially for higher TiO_2 loading, but mainly highly dispersive species with Ti–O–Si linkages at the surface prepared by SSG. These results are well consistent with the XRD analysis. The XPS ratio of Ti 2p/Si 2p was listed in Table 1, which can be used to estimate the TiO_2 loading amount by the SSG method as compared to those obtained from the IMP method.

The XPS Au 4f 7/2 was observed at 83.0–84.2 eV for both TiO_2 and TiO_2/SiO_2 supported catalysts, which binding energy is identical to metallic gold of ~84.0 eV [1,10,18]. Furthermore, Cl was detected by XPS on the as prepared samples but not on the samples after high temperature reduction. It is worth to note that the catalytic activities for Au/TiO_2 and $Au/TiO_2/SiO_2$ prepared using $HAuCl_4$ as a precursor are sensitive to the reduction procedures, especially H_2O amount in hydrogen. The hydrogen used contains ~3 ppm of H_2O. When hydrogen was used to reduce supported $HAuCl_4$ directly, good catalytic activity can be achieved. However, when the hydrogen was further cleaned by trapped in liquid nitrogen in advance, the reduced supported Au catalysts showed barely CO oxidation activity. It is very possible that such small amount of water in hydrogen may aid to remove the chloride and reduction of gold, via hydrolyzing $HAuCl_4$ into $Au(OH)_x$ or AuO_x.

3.2.4. Physical property measurement

Nitrogen physisorption measurements were conducted for TiO_2, SiO_2 and TiO_2/SiO_2 supports. The pore structure parameters, such as BET surface area and cumulative pore volume are listed in Table 1. The pore size distribution of the samples SiO_2, 8 wt% TiO_2/SiO_2(IMP) and TiO_2/SiO_2 (SSG) with two cycles is shown in Fig. 7(A). It is clear that the surface area and pore volume decrease with increasing TiO_2 loading or the repeating cycling number in SSG method. The pore size distribution for the samples prepared by the IMP method is almost identical to SiO_2, but shift to smaller pore sizes for the samples prepared by the SSG method. Such results display that TiO_2 prepared by IMP mainly forms crystalline particles located on the surface, while that by SSG forms a think layer coated on both the external and internal surfaces of SiO_2. This is consistent with the XRD and XPS measurements.

3.2.5. TEM measurement

Transmission electron microscope (TEM) was used to characterize gold nanoparticles on TiO_2. The TEM images for a 2 wt% Au/TiO_2 and 2 wt% $Au/TiO_2/SiO_2$ after H_2 reduction were compared in Fig. 8. Gold nanoparticles are well dispersed on both the TiO_2 and TiO_2/SiO_2 (SSG) surfaces with sizes of 2–12 nm. However, it is more rich of small Au nanoparticles on the TiO_2/SiO_2 (SSG) than that on the TiO_2. This is clear shown by the comparison of the distribution of gold nanoparticles on the both supports in Fig. 8. The Au particles size ranges from 2 to 11 nm with a maximum at 5–7 nm on TiO_2, while from 2 to 8 nm with a maximum at about 3 nm on TiO_2/SiO_2 (SSG). The significantly higher activities for CO oxidation on $Au/TiO_2/SiO_2$ compared to that on TiO_2 can be explained as the rich of Au nanoparticles at a size of about 3 nm, which is the size exhibiting the highest activity observed both on the high-surface-area-support and model TiO_2(1 1 0) surfaces [10,11,17,18].

3.2.6. In situ FTIR studies

CO adsorption was performed by Fourier transform infrared spectroscopy using a home-made *in situ* IR cell [45]. The sample of about 10 mg was well grinded and crushed into a 10 mm diameter translucent disc. The disc was sat in a quartz tube liner IR cell, through which the beam of the spectrometer can pass. The *in situ* IR cell was first pumped down to below 0.1 Torr at room temperature, then shift to H_2 purge. Under H_2 purge, the sample was ramped up in 1 h to a set reduction temperature and maintained the temperature for 3 h, then cool down to room temperature in H_2. Then the IR

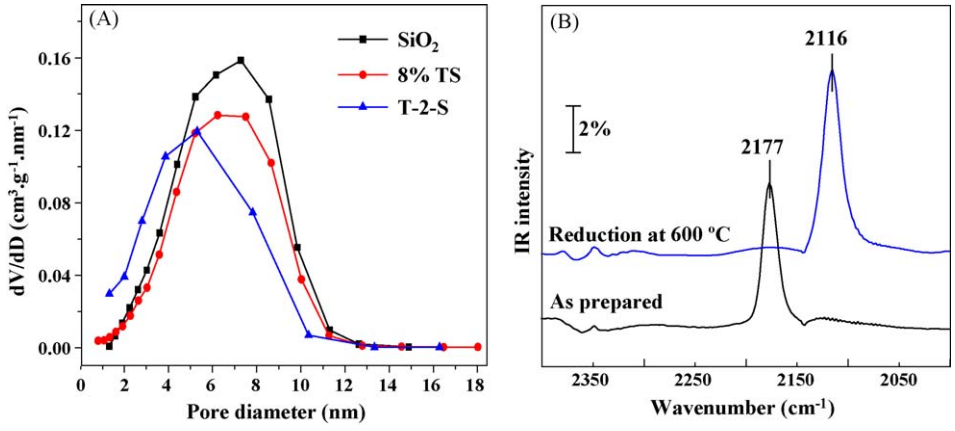

Fig. 7. (A) Pore size distribution for the SiO_2 and TiO_2/SiO_2 prepared by both the IMP and SSG methods. (B) Infrared adsorption spectra of CO on $HAuCl_4/TiO_2/SiO_2$ as prepared and after reduction at 600 °C in H_2.

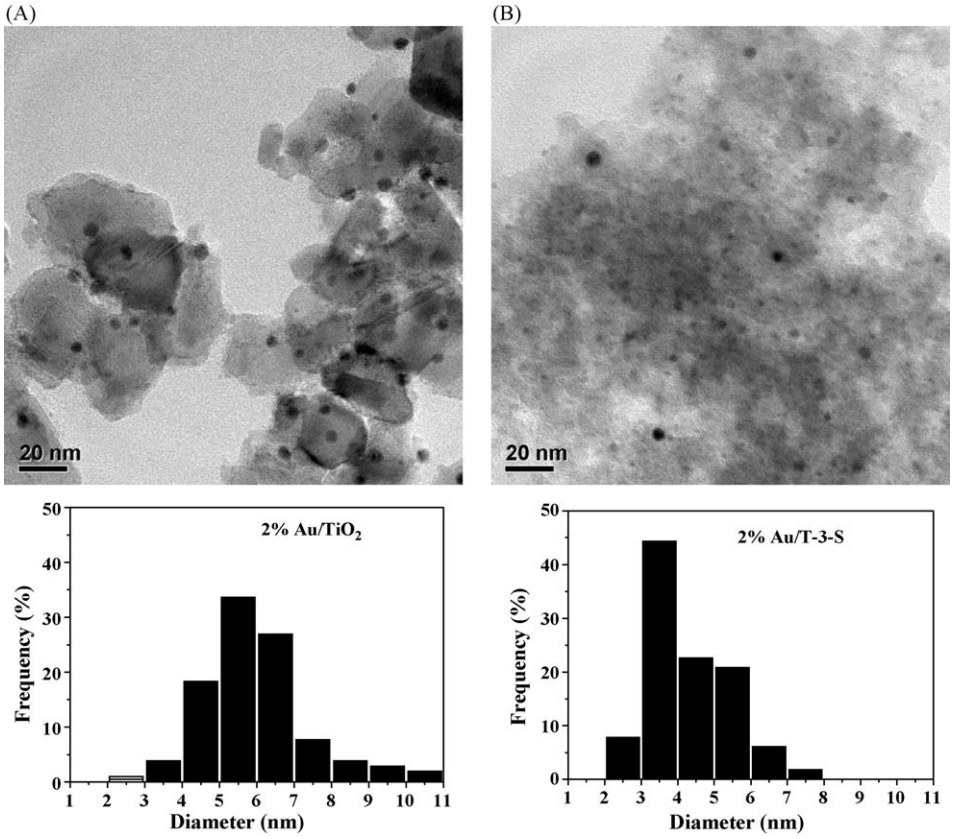

Fig. 8. TEM images and size distribution of Au nanoparticles for (A) 2 wt% Au/TiO_2 and (B) 2 wt% $Au/TiO_2/SiO_2$. The support, TiO_2/SiO_2, was prepared by the SSG method.

cell was pumped down to below 0.1 Torr and several background spectra were taken. High purity CO gas was further cleaned by a liquid nitrogen trap, then introduced into the IR cell of about 1 Torr. IR spectra were taken at room temperature with a certain amount of CO exposing pressures and subtracted the background spectrum taken under vacuum condition. The obtained adsorption spectra were displayed in Fig. 7(B).

The $HAuCl_4/TiO_2/SiO_2$ sample dried at 100 °C distinguishes a main peak at 2177 cm^{-1} from the gas phase CO peaks. This frequency is much higher than CO adsorption on a bulk gold surface of ~2124 cm^{-1} [51]. Thus it can be assigned to CO a-top on a Au^{3+} [52]. After 600 °C reduction treatment, a feature at 2116 cm^{-1} appears. This feature can be assigned to CO a-top on a metallic gold surface [18], consistent with Au 4f binding energy observed at XPS corresponding to metallic gold. As compared to CO adsorbed on bulk gold surface at a frequency of ~2124 cm^{-1}, the feature observed at 2116 cm^{-1} suggests a slightly electron rich metallic gold for $Au/TiO_2/SiO_2$ reduced at 600 °C in H_2 [18,53]. This frequency of 2116 cm^{-1} is close to those of ~2115 cm^{-1} observed for Au/TiO_2(1 1 0) [54] and Au/TiO_2 [55], but higher than that of 2107 cm^{-1} observed for the (1 × 1)-Au/TiO_x/Mo(1 1 2) [20]. Such comparisons reveal that high temperature reduction induces a slightly electron rich metallic gold, which means defects on TiO_2 were created and enriched at the interfaces between gold nanoparticles and TiO_2 surfaces during the deep reduction. As proposed by Rodriguez et al. [56], gold nanoparticles can promote enrich of defect underneath.

3.3. Stability of $Au/TiO_2/SiO_2$ catalysts

The above detailed characterization shows that using the SSG method can coat a thin layer of TiO_2 onto a SiO_2 support, while the IMP method leads to the formation of crystalline TiO_2 on SiO_2. Both kinds of TiO_2/SiO_2 supports enhance the gold catalytic activities for CO oxidation as compared to that for Au on TiO_2. Especially for Au on TiO_2/SiO_2 (SSG), the activity is three times higher than that for Au on TiO_2, which may mainly be owing to the formation of the smaller Au particles as shown in TEM images (Fig. 8).

In the next, the stability of the supported Au catalysts was evaluated, as shown in Fig. 9. The life-time evaluations for Au/TiO_2 and $Au/TiO_2/SiO_2$ both display an initial rapid decrease of the activity, then turns to a relatively stable period. Such rapid deactivation can be regenerated mostly by following a H_2 purge at room temperature (Fig. 9(A)). Thus, the rapid deactivation can be explained as the formation of an inactive carbonate species, which regeneration in H_2 purge is reported to the formation of surface OH that reacts with and remove the surface carbonate species [57]. Beside the rapid deactivation, there is also a slow decrease of the stable activities, which can be considered as an intrinsic deactivation, probably due to the sintering of Au nanoparticles.

As compared Au on TiO_2 and TiO_2/SiO_2 (Fig. 9(A)), $Au/TiO_2/SiO_2$ shows a little slow decrease of the stable activity as indicated by the guide line shown in Fig. 9(A). Moreover, the $Au/TiO_2/SiO_2$ exhibits more than four times higher stable activity that that of the Au/TiO_2. To better evaluate the stability of Au catalysts, the catalytic performances for CO oxidation were measured at 80 °C, at which temperature carbonate species may not involve in the deactivation. The results are shown in Fig. 9(B). Au/TiO_2 still shows a fast decrease of the CO_2 formation rate, with a rate decrease of about 50% within the first 10 h. In contrast, the CO_2 formation rate on $Au/TiO_2/SiO_2$ drops off slowly, with a decrease of less than 20% of the initial rate in 10 h. Such results conclude the significant promotion effects of the dispersion of TiO_2 on SiO_2 on the stability of supported Au cata-

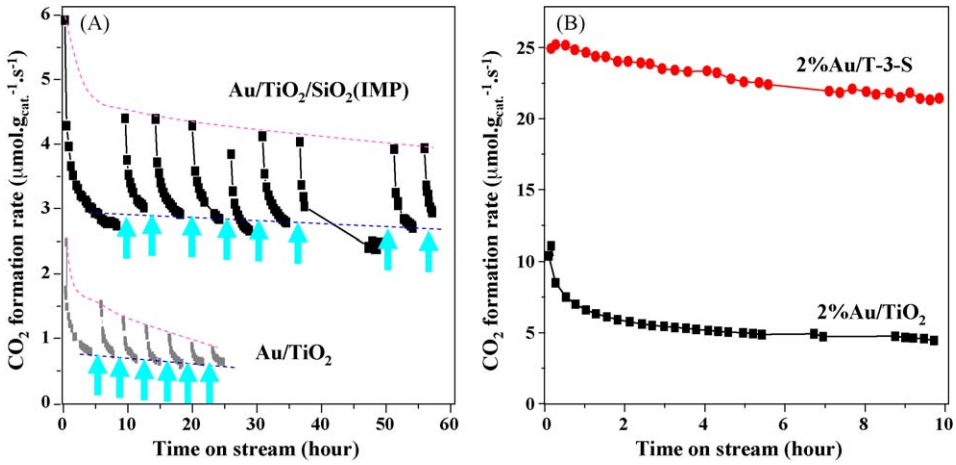

Fig. 9. CO oxidation activities as a function of the reaction time. (A) On 2 wt% Au/TiO_2 and 5 wt% $Au/10$ wt% TiO_2/SiO_2 at room temperature with a hydrogen purge for 30 min each as indicated by arrows and (B) on 2 wt% Au/TiO_2 and 2 wt% $Au/1TiO_2/SiO_2$ (SSG) at 80 °C.

lysts and the activities for CO oxidation. The promotion effects may mainly come from the better dispersion of small Au nanoparticles on a thin layer or small crystalline particles of TiO_2 anchored on SiO_2, leading to sinter resisting.

4. Conclusions

The significant enhancement of catalytic activity for CO oxidation on Au/TiO_2 was achieved by dispersing TiO_2 onto a high-surface-area SiO_2. TiO_2/SiO_2 prepared by the surface sol–gel method possesses a higher activity and better dispersion of TiO_2 on SiO_2 than that by the conventional impregnation method. High temperature reduction at 500–600 °C by H_2 is required to activate the $HAuCl_4$/support precursors. 2 wt% Au supported on the TiO_2/SiO_2 (SSG) forms metallic Au nanoparticles with a size mainly of 3–4 nm, and exhibits about three times higher catalytic activity for CO oxidation than that for Au on TiO_2. Moreover, the stability of Au nanoparticles is apparently enhanced by dispersing TiO_2 on SiO_2 using both the impregnation and surface sol–gel method.

Acknowledgements

The authors thank gratefully the financial support by National Natural Science Foundation of China (20873109), National basic research program of China (973 program: 2005CB221401, 2010CB732303), Major Project of Chinese Ministry of Education (No: 309019). The Ph.D. programs foundation of Chinese Ministry of Education (No. 200803841011) and Natural Science Foundation of Fujian Province, China (2008J0168).

References

[1] M. Haruta, T. Kobayashi, H. Sano, N. Yamada, Chem. Lett. 2 (1987) 405–408; M. Haruta, S. Tsubota, T. Kobayashi, H. Kageyama, M.J. Genet, J. Catal. 144 (1993) 175–192.
[2] B. Nkosi, N.J. N.J. Coville, G.J. Hutchings, J. Chem. Soc. Chem. Commun. 1 (1988) 71–72.
[3] W.A. Bone, G.W. Andrew, Proc. R. Soc. Lond. A 109 (1925) 459.
[4] N.W. Cant, P.W. Frederickson, J. Catal. 37 (1975) 531.
[5] T. Hayashi, K. Tanaka, M. Haruta, J. Catal. 2 (1998) 566–575.
[6] H.W. Yang, D.L. Tang, X.N. Liu, Y.Z. Yuan, J. Phys. Chem. C 113 (2009) 8186–8193.
[7] T.M. Salama, R. Ohnishi, M. Ichikawa, Chem. Commun. 1 (1997) 105–106.
[8] X.K. Wang, A.Q. Wang, X.D. Wang, X.F. Yang, T. Zhang, Gold Bull. 1 (2007) 52–58.
[9] D. Andreeva, V. Idakiev, T. Tabakova, L. Ilieva, P. Falaras, A. Bourlinos, A Travlos, Catal. Today 72 (2002) 51–57.
[10] M. Valden, X. Lai, D.W. Goodman, Science 281 (1998) 1647–1650.
[11] M. Haruta, Catal. Today 36 (1997) 153–166.
[12] Y. Wu, K.Q. Sun, J. Yu, B.Q. Xu, Phys. Chem. Chem. Phys. 10 (2008) 6399–6404.
[13] A.S.K. Hashmi, G.J. Hutchings, Angew. Chem. Int. Ed. 45 (2006) 7896.
[14] J. Schwank, Gold Bull. 16 (1983) 103.
[15] M.M. Schubert, S. Hackenberg, A.C.V. Veen, M. Muhler, V. Plzak, R.J. Behm, J. Catal. 197 (2001) 113–122.
[16] A. Sanchez, S. Abbet, U. Heiz, W.D. Schneider, H. Hakkinen, R.N. Barnett, U. Landman, J. Phys. Chem. C 48 (1999) 9573–9578.
[17] M.S. Chen, D.W. Goodman, Top. Catal. 44 (2007) 41–47.
[18] M.S. Chen, D.W. Goodman, Catal. Today 111 (2006) 22–33.
[19] M.S. Chen, D.W. Goodman, Acc. Chem. Res. 39 (2006) 739–746.
[20] M.S. Chen, D.W. Goodman, Chem. Soc. Rev. 37 (9) (2008) 1860–1870.
[21] M.S. Chen, D.W. Goodman, Science 306 (2004) 252–255.
[22] G.R. Bamwenda, S. Tsubota, T. Nakamura, M. Haruta, Catal. Lett. 44 (1997) 83–87.
[23] S. Ivanova, C. Petit, V. Pitchon, Appl. Catal. A 267 (2004) 191–201.
[24] X.F. Lai, D.W. Goodman, J. Mol. Catal. A 162 (2000) 33–50.
[25] R.M. Rioux, H. Song, J.D. Hoefelmeyer, P. Yang, G.A. Somorjai, J. Phys. Chem. B 109 (2005) 2192–2202.
[26] X.Q. Huang, C.Y. Guo, J.Q. Zuo, N.F. Zheng, G.D. Stucky, Small 3 (2009) 361–365.
[27] C.M. Wang, K.N. Fan, Z.P. Liu, J. Phys. Chem. C 111 (2007) 13539–13546.
[28] N.W. Can, N.J. Ossipoff, Catal. Today 36 (1997) 125–133.
[29] L. Guczi, D. Horvath, Z. Paszti, G. Peto, Catal. Today 72 (2002) 101–105.
[30] A.C. Gluhoi, B.E. Nieuwenhuys, Catal. Today 122 (2007) 226–232.
[31] C.N. Kuo, H.F. Chen, J.N. Lin, B.Z. Wan, Catal. Today 122 (2007) 270–276.
[32] W.F. Yan, S.M. Mahurin, Z.W. Pan, S.H. Overbury, S. Dai, J. Am. Chem. Soc. 127 (2005) 10480–10481.
[33] K. Qian, S.S. Lv, X.Y. Xiao, H.X. Sun, J.Q. Lu, M.F. Luo, W.X. Huang, J. Mol. Catal. A 306 (2009) 40–47.
[34] B.K. Min, W.T. Wallace, D.W. Goodman, J. Phys. Chem. B 108 (2004) 14609–14615.
[35] H.G. Zhu, Z. Ma, S.H. Overbury, S. Dai, Catal. Lett. 116 (2007) 128–135.
[36] K. Qian, W.X. Huang, Z.Q. Jiang, H.X. Sun, J. Catal. 248 (2007) 137–141.
[37] Z. Ma, S.H. Overbury, S. Dai, J. Mol. Catal. A 273 (2007) 186–197.
[38] M. Venezia, F.L. Liotta, G. Pantaleo, A. Beck, A. Horváth, O. Geszti, A. Kocsonya, L. Guczi, Appl. Catal. A 310 (2006) 114–121.
[39] L. Guczi, K. Frey, A. Beck, G. Petõ, C.S. Daróczi, N. Kruse, S. Chenakin, Appl. Catal. A 291 (2005) 116–125.
[40] K. Qian, W.X. Huang, J. Fang, S.S. Lv, B. He, Z.Q. Jiang, S.Q. Wei, J. Catal. 255 (2008) 269–278.
[41] Horváth, A. Beck, A. Sárkóny, G. Stefler, Z. Varga, O. Geszti, L. Tóth, L. Guczi, J. Phys. Chem. B 110 (2006) 15417–15425.
[42] M.A.P. Dekkers, M.J. Lippits, B.E. Nieuwenhuys, Catal. Today 54 (1999) 381–390.
[43] I. Ichinose, H. Senzu, T. Kunitake, Chem. Mater. 9 (1997) 1296–1298.
[44] M. Cozzolino, M.D. Serio, R. Tesser, E. Santacesaria, Appl. Catal. A 325 (2007) 256–262.
[45] W.Z. Weng, M.S. Chen, H.L. Wan, Chem. Rec. 2 (2002) 102.
[46] X.T. Gao, I.E. Wachs, Catal. Lett. 51 (1999) 233–254.
[47] A. Fernandez, J. Leyrer, A.R. González-Elipe, G. Munuera, H. Knözinger, J. Catal. 112 (1988) 489–494.
[48] A.Y. Stakheev, E.S. Shpiro, J. Apijok, J. Phys. Chem. 97 (1993) 5668–5672.
[49] R. Castillo, B. Koch, P. Ruiz, B. Delmon, J. Catal. 161 (1996) 524–529.
[50] X.T. Gao, S.R. Bare, J.L.G. Fierro, J. Phys. Chem. B 102 (1998) 5653–5666.
[51] D.C. Meier, V. Bukhtiyarov, D.W. Goodman, J. Phys. Chem. B 126 (2003) 12668–12671.
[52] F. Boccuzzi, A. Chiorino, M. Manzoli, P. Lu, T. Akita, S. Ichikawa, M. Haruta, J. Catal. 202 (2001) 256–267.

[53] M. Sterrer, M. Yulikov, E. Fischbach, M. Heyde, H.P. Rust, G. Pacchioni, T. Risse, H.J. Freund, Angew. Chem. Int. Ed. 45 (2006) 2630–2632.
[54] M. Chen, Y. Cai, Z. Yan, D.W. Goodman, J. Am. Chem. Soc. 128 (2006) 6341–6346.
[55] M. Haruta, M. Date, Appl. Catal. A 222 (1–2) (2001) 427–437.
[56] J.A. Rodriguez, G. Liu, T. Jirsak, J. Hrbek, Z.P. Chang, J. Dvorak, A. Maiti, J. Am. Chem. Soc. 124 (2002) 5242–5250.
[57] H.S. Oh, C.K. Costello, C. Cheung, H.H. Kung, M.C. Kung, Stud. Surf. Sci. Catal. 139 (2001) 375.